Nuclear Engineering and Technology 56 (2024) 2120–2130

Contents lists available at ScienceDirect

Nuclear Engineering and Technology

journal homepage: www.elsevier.com/locate/net

Original Article

An efficient seismic analysis technique for PCSG assembly using sub-structuring method and homogenization method

Gyogeun Youn [a], Wanjae Jang [b], Gyu Mahn Lee [a], Kwanghyun Ahn [a], Seongmin Chang [c,*]

[a] SMART System Development Division, Korea Atomic Energy Research Institute, 111, Daedeok-daero 989beon-gil, Yuseong-gu, Daejeon, 34057, Republic of Korea
[b] Department of Mechanical Engineering, Kumoh National Institute of Technology, 61, Daehak-ro, Gumi-si, Gyeongsangbuk-do, 39177, Republic of Korea
[c] School of Mechanical Engineering, Chungnam National University, 99, Daehak-ro, Yuseong-gu, Daejeon, 34134, Republic of Korea

ARTICLE INFO

Keywords:
PCSG assembly
Efficient seismic analysis technique
Sub-structuring method
Homogenization method

ABSTRACT

This study significantly reduced the seismic analysis time of PCSG assembly by introducing a reduced model using homogenization and sub-structuring methods. The homogenization method was applied to the primary and secondary micro-channel sheets, and the sub-structuring method was applied to the PCSG module sets. Modal analysis and frequency response analysis were then performed to validate the accuracy of the reduced model. The analysis results were compared with the full model and it was confirmed that the reduced model provided almost the same analysis results as the full model. To verify the computational efficiency of the reduced model, the computational time was then compared with the full model, and it was confirmed that the modal analysis time was reduced by 3.42 times and the frequency response analysis time was reduced by 4.59 times.

1. Introduction

SMRs (Small Modular Reactors) are becoming a recent trend due to their advantages in safety, cost-effectiveness, sustainability, flexibility, and adaptability [1]. However, to harness these benefits, it is crucial to design SMRs with compact sizes. For this purpose, it is important to maximize the heat transfer area per unit volume in the steam generator.

Recently developed SMRs such as NuScale [2] or Westinghouse [2] commonly employ a helical coil design in the steam generator to enhance heat transfer efficiency. On the other hand, due to its higher heat transfer efficiency compared to a helical steam generator [3], the PCSG (Printed Circuit Steam Generator) has garnered significant attention in research efforts to apply it to SMRs or Gen IV reactors. PCSG is a steam generator made by alternately stacking primary coolant micro-channel sheets and secondary coolant micro-channel sheets. The PCSG's superior heat transfer efficiency allows for the design of more compact SMRs. As a result, there have been diverse research studies exploring the application of PCSG in SMRs or Gen IV reactors [4–11].

However, existing studies have been focused on verifying the thermal-hydraulic performance of PCSG or evaluating the structural integrity of unit micro-channel. Due to the numerous micro-channels formed by alternating layers of primary and secondary coolant micro-channel sheets, conducting a structural integrity evaluation by accurately reflecting the micro-channel geometry in the PCSG unit block is time-consuming and not cost effective. Therefore, in our previous study [12], we proposed a method to effectively evaluate the structural integrity of PCSG unit block by applying the homogenization method.

The homogenization method [12–19] converts an inhomogeneous elastic body into a homogeneous elastic body with same mechanical behaviour. Applying this method has the advantage of being able to efficiently express the mechanical behaviour of PCSG unit block that contain unit micro-channels that are repeated in large numbers in the same pattern.

This paper proposes a method to efficiently perform the seismic analysis of PCSG assembly by extending our previous study [12]. The PCSG assembly has a structure in which PCSG module sets, formed by stacking several PCSG unit blocks, are repeated in a circular pattern. Therefore, for the PCSG assembly composed of dozens of PCSG unit blocks, it is difficult to perform the analysis by reflecting all the shapes of numerous micro-channels. Thus, we propose a method to perform the seismic analysis of PCSG assembly by applying the sub-structuring method along with the homogenization method proposed in our previous study [12]. Note that seismic analysis is much more time consuming than static analysis because it considers cyclic loading.

Sub-structuring method [20–27] is one of the methods that can effectively analyze large structures with repetitive patterns. The sub-structuring method is a method of analyzing a part of a structure

* Corresponding author.
E-mail address: schang@cnu.ac.kr (S. Chang).

https://doi.org/10.1016/j.net.2024.01.020
Received 23 November 2023; Received in revised form 10 January 2024; Accepted 14 January 2024
Available online 20 January 2024

Nomenclature

φ_N	matrix of retained normal modes of sub-structure
φ_C	matrix of constraint modes of sub-structure
φ_{c-b}	CB transformation matrix
C	damping matrix
D_H	equivalent elastic constants
$F(t)$	external force depending on time
I	identity matrix
K	stiffness matrix
K_{bb}	boundary stiffness matrix
M	mass matrix
M_{bb}	boundary mass matrix
q	system generalized coordinates
t	time
u	degrees of freedom
ξ	damping ratio
ω	natural frequency

Abbreviation

CB	Craig and Bampton
CMS	Component Mode Synthesis
DOF	Degree of Freedom
FE	Finite Element
Gen IV	Generation IV
PCSG	Printed Circuit Steam Generator
SMR	Small Modular Reactor

after dividing it into each sub-structure, and using the analysis result to determine the characteristics of the entire structure. Among the sub-structuring methods, CMS (Component Mode Synthesis) methods are commonly utilized to describe numerical models by reducing physical systems focusing on their most dominant dynamic behaviors. The advantage of CMS methods is that they allow the description of internal DOFs (Degrees of Freedom) within the physical domain using modes, while keeping the interface in their physical form.

CMS methods are divided into fixed interface CMS method and free interface CMS method. The free interface CMS method is more applicable than the fixed interface method, but is less accurate due to its weaker interface. Thus fixed interface CMS method is considered in this research. Hurty [28] and Guyan [29] first proposed the fixed interface CMS method, where global eigen-solutions are projected onto the subspace formed by sub-structural constraint modes and fixed normal modes. Craig and Bampton [30] later simplified this method by categorizing interface forces into statically determinate and indeterminate components. This streamline approach is widely employed for efficient and comprehensible eigenvalue solutions. Capitalizing on these advantages, we incorporated the CB (Craig and Bampton) method, already well-established in aerospace and mechanical fields [31–33], although it is presently not extensively utilized in the nuclear domain [34].

Section 2 explains the theoretical background of the CB method. Section 3 describes the procedure for applying the sub-structuring method to the PCSG assembly. Then, modal analysis and frequency response analysis were performed to verify the validity of the reduced model to which the homogenization method and sub-structuring method were applied. Section 4 discusses the computational efficiency of the reduced model. Section 5 concludes the presented work.

2. Review OF CB (CRAIG and BAMPTON) SUB-STRUCTURING method

The CB (Craig and Bampton) method [30] is one of the sub-structuring methods and is widely used in many commercial programs. This is a hybrid reduction method in which the degree of freedom corresponding to the contact area with other parts in the sub-structure is reduced using the degree-of-freedom-based reduction method, and the remaining area is reduced using the mode-based reduction method.

Using the sub-structuring method, the entire finite element model can be recreated as a reduced finite element model. To this end, only the parts to be considered in the analysis are left, and the remaining parts are replaced with sub-structures. However, unlike dynamic analysis, in static analysis, sub-structuring method can be used without errors. As a result, the sub-structure can be treated as if it were one large element, so it is also referred to as a super element.

In the dynamic equations, the total degrees of freedom of the system u_A can be expressed as follows.

$$[M_{AA}]\left\{\ddot{u}_A\right\} + [C_{AA}]\{\dot{u}_A\} + [K_{AA}]\{u_A\} = \{F(t)\} \tag{1}$$

where $[M]$ denotes mass matrix, $[C]$ denotes damping matrix, $[K]$ denotes stiffness matrix, and $\{F(t)\}$ denotes external force vector depending on time t. Note that the subscript A stands for 'total'.

For matrix reduction, the total degrees of freedom can be divided into the degrees of freedom at boundary u_B (the region of interest) and the degrees of freedom at interior u_L (excluding the region of interest) as follows.

$$\begin{bmatrix} M_{BB} & M_{BL} \\ M_{LB} & M_{LL} \end{bmatrix} \begin{Bmatrix} \ddot{u}_B \\ \ddot{u}_L \end{Bmatrix} + \begin{bmatrix} C_{BB} & C_{BL} \\ C_{LB} & C_{LL} \end{bmatrix} \begin{Bmatrix} \dot{u}_B \\ \dot{u}_L \end{Bmatrix} + \begin{bmatrix} K_{BB} & K_{BL} \\ K_{LB} & K_{LL} \end{bmatrix} \begin{Bmatrix} u_B \\ u_L \end{Bmatrix} = \begin{Bmatrix} F_B \\ F_L \end{Bmatrix} \tag{2}$$

Note that subscripts B and L refer to boundary and interior, respectively.

The CB transformation matrix φ_{c-b} is defined as follows.

$$\varphi_{c-b} = \begin{bmatrix} I & 0 \\ \varphi_C & \varphi_N \end{bmatrix} \tag{3}$$

where φ_C denotes the matrix of constraint modes of sub-structure, and φ_N denotes the matrix of retained normal modes of sub-structure. Note that I denotes identity matrix.

When the CB transformation matrix is applied to all degrees freedom, the degrees of freedom at boundary u_B and the degrees of freedom at interior u_L are shown in Eq. (4) below.

$$\{u_A\} = \begin{Bmatrix} u_B \\ u_L \end{Bmatrix} = \begin{bmatrix} I & 0 \\ \varphi_C & \varphi_N \end{bmatrix} \begin{Bmatrix} u_B \\ q \end{Bmatrix} \tag{4}$$

Here, q denotes the system generalized coordinates. Through the CB transformation matrix, it can be seen that the degrees of freedom are maintained at the boundary and the degrees of freedom at interior are reduced based on the mode.

Utilizing Eq. (4) to simplify Eq. (2), the resulting dynamic equation indicates that the external force acting on internal degrees of freedom are represented as zero ($F_L = 0$), as shown in the following equation.

$$\begin{bmatrix} M_{bb} & M_{bl} \\ M_{lb} & M_{ll} \end{bmatrix} \begin{Bmatrix} \ddot{u}_B \\ \ddot{q} \end{Bmatrix} + \begin{bmatrix} 0 & 0 \\ 0 & 2\xi\omega \end{bmatrix} \begin{Bmatrix} \dot{u}_B \\ \dot{q} \end{Bmatrix} + \begin{bmatrix} K_{bb} & 0 \\ 0 & \omega^2 \end{bmatrix} \begin{Bmatrix} u_B \\ q \end{Bmatrix} = \begin{Bmatrix} F_B \\ 0 \end{Bmatrix} \tag{5}$$

Here, ω and ξ denote natural frequency and damping ratio, respectively. Furthermore, M_{bb}, M_{bl} and M_{lb} are defined as follows.

$$M_{bb} = \varphi_C^T[M_{LL}\varphi_C + M_{LB}] + M_{BL}\varphi_C + M_{BB} \tag{6}$$

$$M_{bl} = \varphi_C^T M_{LL}\varphi_N + M_{BL}\varphi_N \tag{7}$$

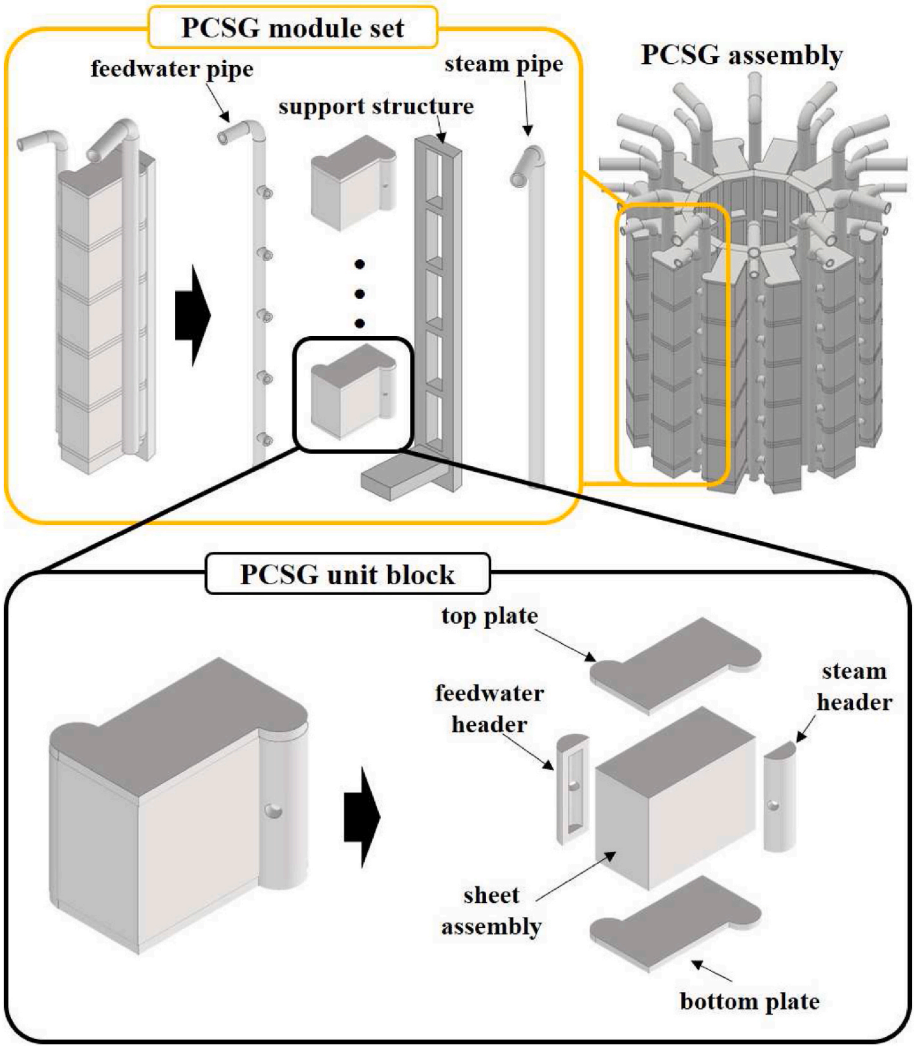

Fig. 1. Components of PCSG assembly.

$$M_{lb} = \varphi_N^T [M_{LL}\varphi_C + M_{LB}] \tag{8}$$

3. Seismic analysis of PCSG assembly

3.1. Creation of a reduced model using sub-structuring and homogenization methods

In this study, PCSG assembly, which has many components with repeating patterns, was used as a numerical example. In order to verify the analysis accuracy of the reduced model using the sub-structuring method, the same analysis was performed on the full model without applying the sub-structuring method.

As shown in Fig. 1, the PCSG assembly used in this study has a structure in which the PCSG module set is repeated 12 times in a circular pattern. Each module set is a 5-layer stack of PCSG unit blocks combined with support structure, feedwater pipe and steam pipe. The PCSG unit block consists of a top plate, bottom plate, sheet assembly, feedwater header and steam header. The top and bottom plates are attached to the top and bottom of the sheet assembly, respectively. The feedwater header is attached to the left side of the sheet assembly, and the steam header is attached to the right side. Note that the sheet assembly in Fig. 1 is a simplified model using the homogenization method.

The overview of creating a reduced model of PCSG assembly is shown in Fig. 2, and a detailed procedure is as follows:

1) Simplifying PCSG unit block modeling with homogenization method.

① Determination of material property input data for PCSG unit block for FE analysis (excluding the sheet assembly)

All components of the PCSG assembly are designed with alloy 690. Accordingly, during FE analysis, all components of the PCSG assembly (excluding sheet assembly) should be analyzed by applying alloy 690 material properties as presented in Table 1 [12,35,36]. However, since the homogenization method is applied to the sheet assembly, the equivalent elastic constants $D^H_{\text{sheet assembly}}$ should be applied instead of alloy 690 properties. Thus, among the 5 components of PCSG unit block (see Figs. 1 and 2), only the remaining components excluding the sheet assembly are subjected to FE analysis using the alloy 690 properties.

② Homogenization of sheet assembly

Sheet assembly is a structure where 1st sheet and 2nd sheet are stacked alternately for hundreds of times, as illustrated in Fig. 3(a). The 1st sheets and 2nd sheets are attached through diffusion bonding, forming the micro-channel shapes depicted in Fig. 3(b) and (c). As shown in Fig. 3(c), 1st sheet is made into a straight type micro-channel, and the 2nd sheet is manufactured as a zigzag type micro-channel [12]. Note that these micro-channel shapes are repeated countless times.

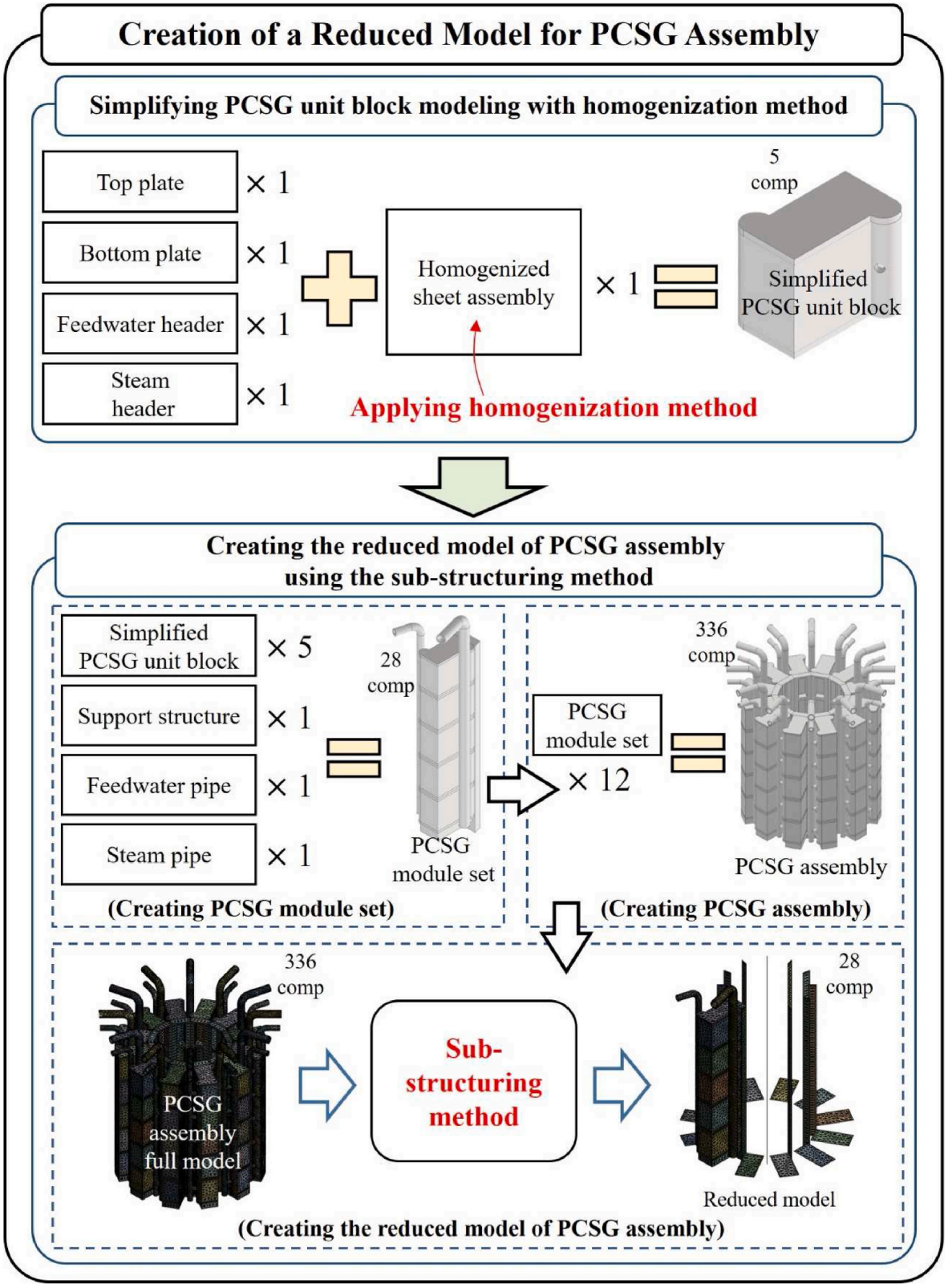

Fig. 2. Overview of creating a reduced model of PCSG assembly.

Homogenization method transforms inhomogeneous elastic body into homogeneous elastic body with same mechanical behavior. This method is effective when dealing with repeated microstructures of inhomogeneous elastic body. Thus, it can be effectively applied to a sheet assembly where micro-channels are repeated countless times, and the procedure is illustrated in Fig. 4.

Firstly, the reference model that reflects the actual geometry of the model in which the 1st and 2nd sheets are stacked is created. Then using the ANSYS material designer option, the equivalent elastic constants of the homogenized model $D^{H}_{\text{sheet assembly}}$ can be obtained (see Table 2),

Table 1
Material properties of alloy 690 at room temperature (25 °C) [12,35,36].

Material properties	Value
Elastic modulus [GPa]	208.0
Shear modulus [GPa]	81.8
Poisson's ratio	0.289
Density [kg/m^3]	8110

providing the same mechanical behavior as the reference model. Note that the procedure for obtaining the equivalent elastic constants $D^H_{\text{sheet assembly}}$ is described in detail in our previous study [12].

③ Creating simplified PCSG unit block

By assembling the remaining components (top plate, bottom plate, feedwater header and steam header) into the homogenized sheet assembly model, a simplified PCSG unit block can be created. The geometry of the simplified PCSG unit block is shown in Figs. 1 and 2.

2) Creating the reduced model of PCSG assembly using substructuring method.

① Creating PCSG module set

As shown in Figs. 1 and 2, the PCSG module set is a structure in which 5 layers of PCSG unit blocks are stacked on a support structure, and then the feedwater and steam pipes are combined. The PCSG module set has a total of 28 components: 5 PCSG unit blocks (A PCSG unit block consists of 5 components), 1 feedwater pipe, 1 steam pipe, and 1 support structure. Note that the PCSG unit block applied here is a simplified PCSG unit block obtained through the homogenization

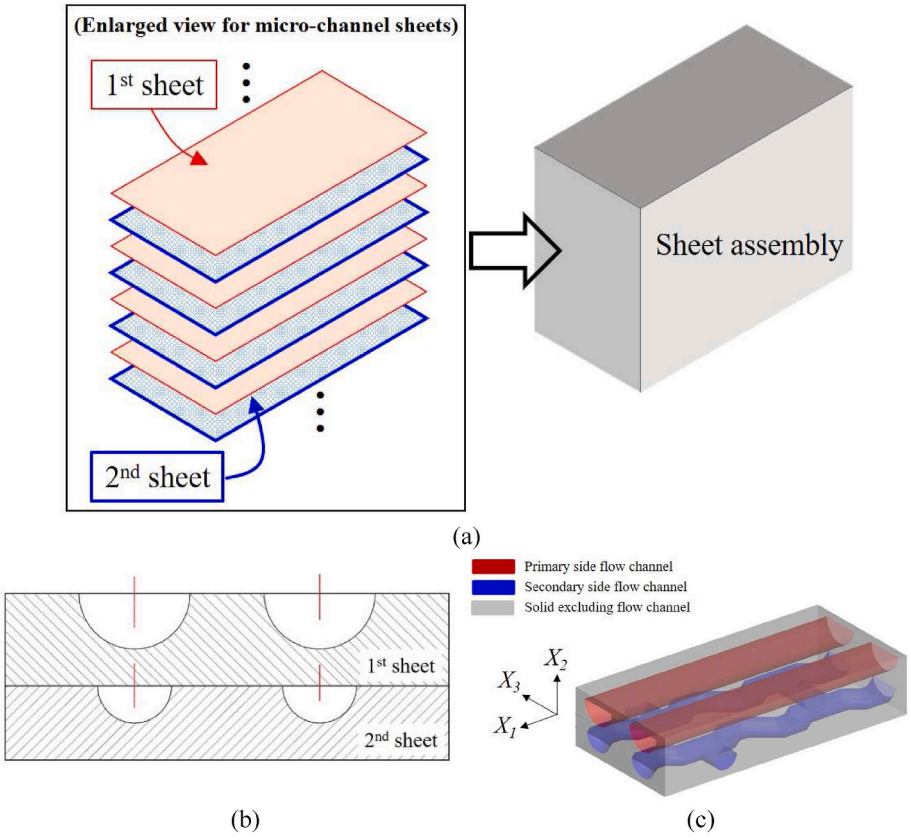

Fig. 3. Structure of sheet assembly (a) overview of the 1st sheet and 2nd sheet stacking (b) front view and (c) iso view of the micro-channel in the 1st sheet and 2nd sheets [12].

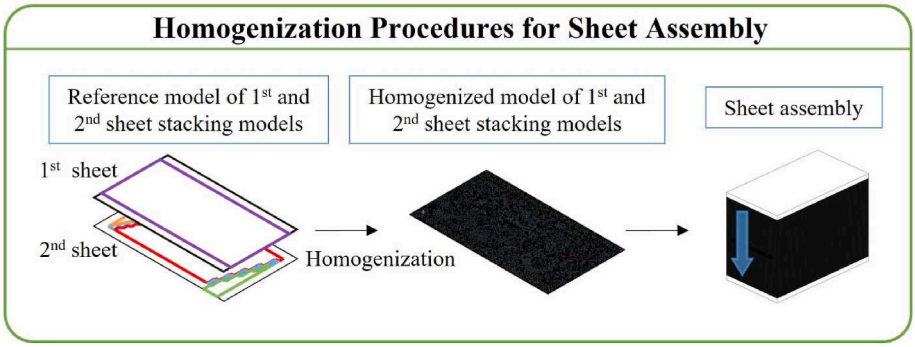

Fig. 4. Homogenization procedures for sheet assembly [12].

Table 2
Equivalent elastic constants of homogenized sheet assembly model ($D^{H}_{\text{sheet assembly}}$) [12].

Material properties		Value
Elastic modulus [GPa]	*X*	165.7
	Y	139.3
	Z	140.9
Shear modulus [GPa]	*XY*	54.3
	YZ	38.9
	ZX	55.9
Poisson's ratio	*XY*	0.281
	YZ	0.231
	ZX	0.282
Density [kg/m^3]		6655.1

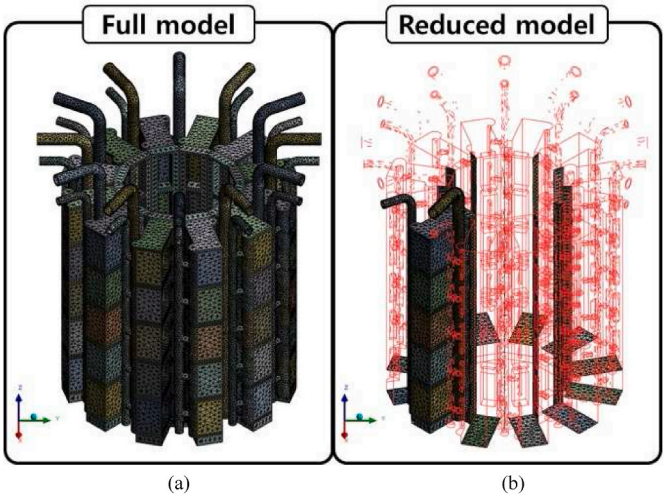

Fig. 5. FE model of PCSG assembly (a) full model and (b) reduced model.

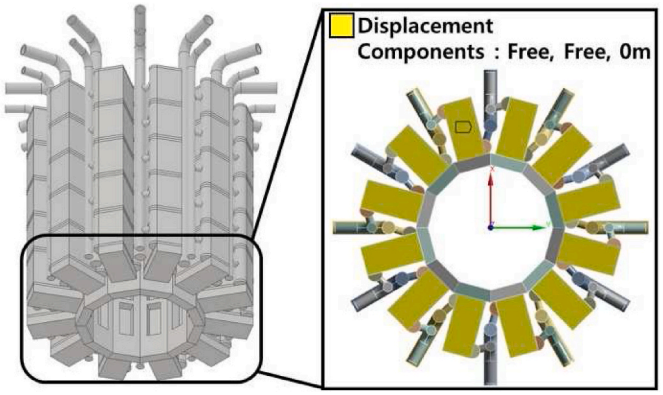

Fig. 6. Boundary conditions for modal analysis of the PCSG assembly.

method.

② Creating the full model of PCSG assembly

The full model of PCSG assembly can be obtained by creating 12 PCSG module sets in a circular pattern. Fig. 5(a) shows the full model of PCSG assembly for FE analysis. The model used tetra 10 elements, and an element size of 4 cm was applied. Note that the full model consists of 12 PCSG module sets, so it consists of 336 components.

③ Creating the reduced model of PCSG assembly using sub-structuring method

Table 3
Comparison of natural frequency between full model and reduced model.

Mode order	Natural Frequency [Hz]		Error (%)
	Full model	Reduced model	
1	38.8047	38.8049	0.0005
2	38.8248	38.8251	0.0008
3	38.8993	38.8993	0
4	38.9026	38.9025	0.0003
5	38.9234	38.9234	0
6	38.9337	38.9338	0.0003
7	38.9433	38.9433	0
8	38.9476	38.9475	0.0003
9	38.9531	38.9529	0.0005
10	39.0590	39.0591	0.0003
11	39.0641	39.0641	0
12	39.2469	39.2472	0.0008
13	47.4656	47.4690	0.0072
14	47.4946	47.4980	0.0072
15	48.1780	48.1782	0.0004

In the reduced model, all but one of the 12 PCSG module sets were replaced with sub-structures (see Fig. 5(b)). Sub-structures can be created using the 'Sub-structure Generation' option provided by ANSYS, a commercial FE analysis program. When creating the reduced model, the mechanical behavior of the full model can be reflected by considering not only the contact area with other components, but also the degree of freedom of the area where load and boundary conditions are to be applied. The full model consists of 336 components, and the reduced model consists of 28 components. Note that the reduced model of PCSG assembly has the same geometry as the PCSG module set, so the number of components is the same.

3.2. Validation of reduced model through modal analysis

In order to identify the vibration characteristics of a structure, ① modal analysis, ② frequency response analysis, and ③ transient response analysis are generally performed. Modal analysis evaluates the natural frequency of the structure under free vibration conditions. Note that the free vibration conditions are an environment without damping ($C = 0$) and external force ($F(t) = 0$) in Eq. (1).

Even if the magnitude of the external force is small, resonance occurs when a load is applied at the same frequency as the natural frequency, which is a critical problem that reduces the integrity of the structure. In general, since the magnitude or the frequency of the external force cannot be controlled, the resonance is avoided by adjusting the natural frequency. Therefore, when applying the sub-structuring method, it is very important to verify that the natural frequency is accurately calculated in the reduced model, and this was done through comparison with the analysis results of the full model.

For both the full model and the reduced model, boundary conditions were imposed on the bottom surface of the structure for modal analysis (see Fig. 6). If the displacement in the *X*, *Y*, and *Z* axes is fixed using the fixed support condition, the structure cannot take into account the displacement caused by ground shaking. To solve this problem, the displacement due to the inertia of the structure and the displacement due to shaking of the ground were considered together by imposing a roller boundary condition on the bottom surface of the structure as shown in Fig. 6.

Table 3 shows the results of comparing the natural frequencies of the full model and reduced model according to mode order. The mode orders were compared by deriving results up to the 15th order mode, excluding the rigid body mode. Even in the 13th and 14th modes, where the natural frequency difference is the largest, the error of the reduced model compared to the full model is 0.0072 %, showing that modal analysis can be performed with very high accuracy with the reduced model.

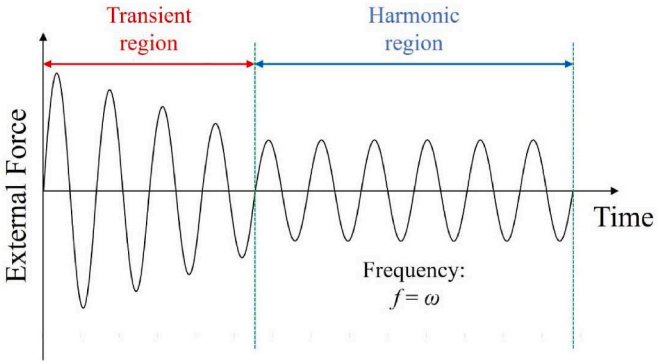

Fig. 7. Schematic drawing of transient region and harmonic region.

3.3. Validation of reduced model through frequency response analysis

In this section, frequency response analysis was performed among ① modal analysis, ② frequency response analysis, and ③ transient response analysis. Frequency response analysis is an analysis that determines the frequency response when a harmonic excitation load ($F(t)$

Table 4
Comparison of frequency response (acceleration at peak point) between full model and reduced model in Case 1.

Axis	Frequency Response Comparison: Acceleration at Peak Point [m/s^2]		Error (%)
	Full Model	Reduced Model	
X	1.3731×10^{-3}	1.3738×10^{-3}	0.05
Y	3.5249×10^{-3}	3.5270×10^{-3}	0.06
Z	1.9335×10^{-4}	1.9355×10^{-4}	0.10

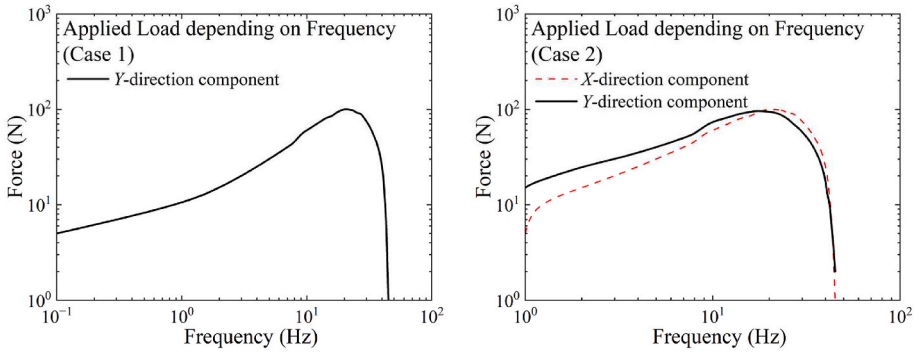

Fig. 8. Frequency domain of applied load (a) Case 1 (b) Case 2.

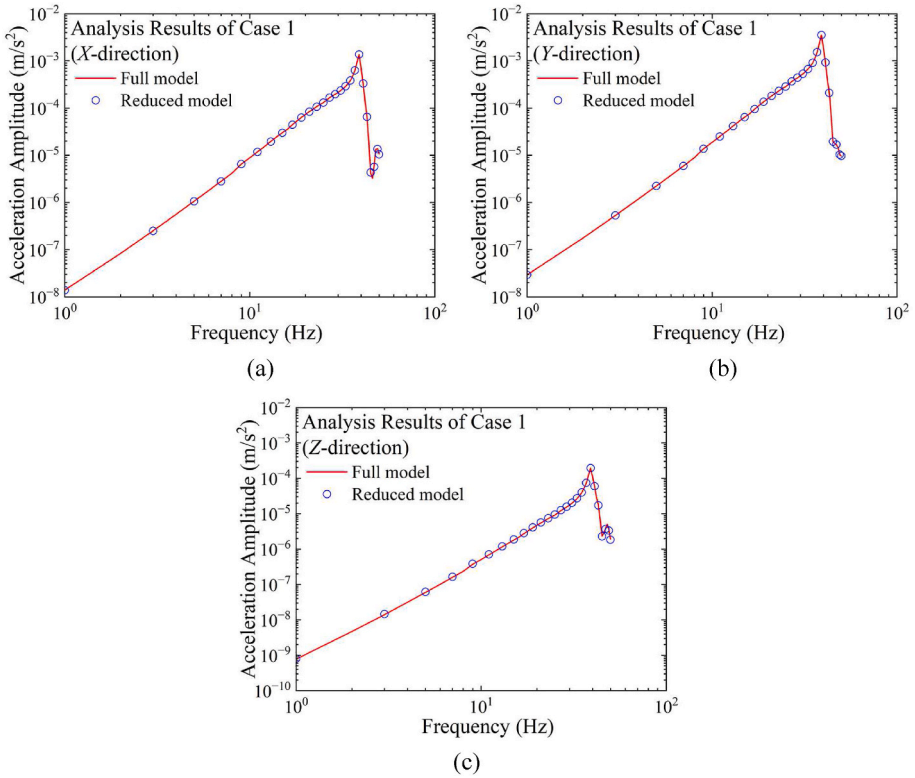

Fig. 9. Comparison of frequency response analysis results (acceleration amplitude) between full model and reduced model in Case 1 (a) X-direction (b) Y-direction (c) Z-direction.

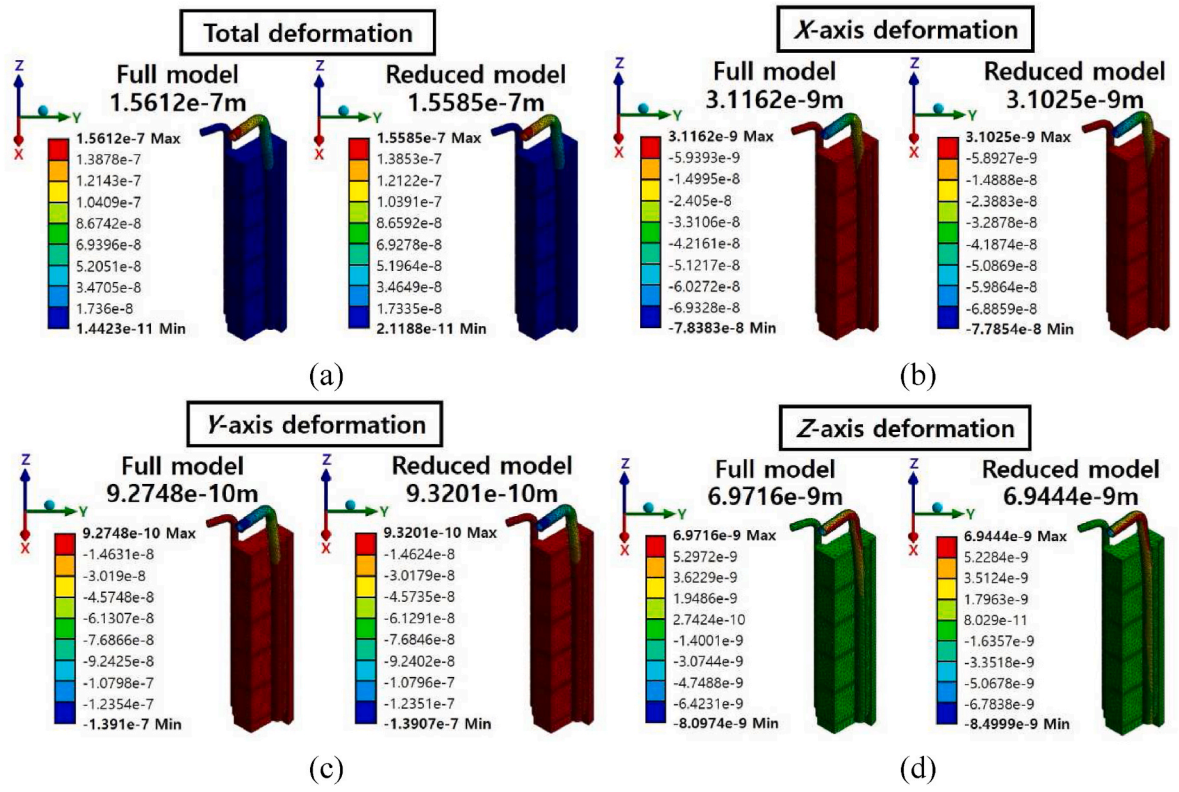

Fig. 10. Analysis results of deformation between full model and reduced model in Case 1 (a) total deformation (b) *X*-axis deformation (c) *Y*-axis deformation (d) *Z*-axis deformation (unit: m).

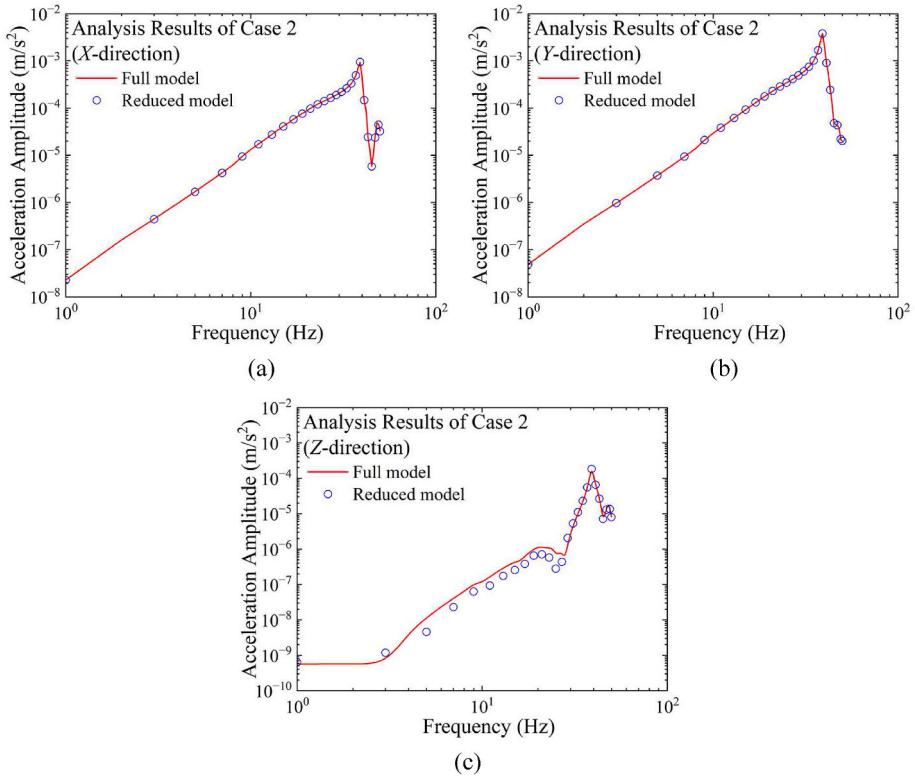

Fig. 11. Comparison of frequency response analysis results (acceleration amplitude) between full model and reduced model in Case 2 (a) *X*-direction (b) *Y*-direction (c) *Z*-direction.

Table 5
Comparison of frequency response (acceleration at peak point) between full model and reduced model in Case 2.

Axis	Frequency Response Comparison: Acceleration at Peak Point [m/s^2]		Error (%)
	Full model	Reduced model	
X	9.4308×10^{-4}	9.4261×10^{-4}	0.05
Y	3.8194×10^{-3}	3.8215×10^{-3}	0.06
Z	1.8424×10^{-4}	1.8441×10^{-4}	0.09

$= F_0 \sin\omega t$) is applied to the external force of Eq. (1). Thus, frequency response analysis is also called harmonic response analysis (see Fig. 7). Note that the analysis is conducted in the frequency domain using FFT (Fast Fourier Transform).

Transient response analysis is an analysis that obtains the response when the external force in Eq. (1) is given arbitrarily over time (see Fig. 7). Therefore, transient response analysis should be performed by reflecting the time history. Note that transient response analysis was not performed in this research because this level of detailed analysis is not required at the design stage.

To perform frequency response analysis for the two cases, the external force depending on frequency was applied as shown in Fig. 8. The load is applied to the bottom surface of the model the same as the boundary conditions in Fig. 6. To compare the seismic analysis results under various loading conditions, analysis was performed for Case 1, in which the load applied only in the *Y*-direction, and Case 2, in which the load applied in both *X* and *Y* directions. Note that damping is not considered ($C = 0$) in these analyses.

The frequency response results of the full model and reduced model for Case 1 are shown in Fig. 9. The horizontal axis of the graph represents the frequency and the vertical axis represents the acceleration amplitude, and it can be seen that the results of the reduced model matches well with the results of the full model. Table 4 compares the maximum acceleration amplitude of the full model and the reduced model for Case 1. As can be seen in Fig. 9, the maximum acceleration amplitude in all *X*, *Y*, and *Z* directions is at a frequency of 39 Hz. Thus, the acceleration amplitudes at 39 Hz were compared. It can be seen that even in the case of the *Z* direction, which showed the largest difference, the error is only 0.1 %, showing that the accuracy of the reduced model is very high.

Fig. 10 compares the displacement of the full model and the reduced model when the frequency is 39 Hz under Case 1 loading conditions. The total deformation (Fig. 10(a)) is 1.5612×10^{-7} m for the full model and 1.5585×10^{-7} m for the reduced model, with an error of only about 0.17 %. When comparing the displacements of the full model and the reduced model in each direction, errors of 0.44 % in *X* direction, 0.49 % in *Y* direction, and 0.39 % in *Z* direction occur, indicating that the displacements of the two models are almost the same.

The frequency response results of the full model and reduced model for Case 2 are shown in Fig. 11, and it can be seen that the results of the reduced model match well with the results of the full model. Table 5 compares the maximum acceleration amplitude of the full model and the reduced model for Case 2. As can be seen in Fig. 11, the maximum acceleration amplitude is at the frequency of 39 Hz in all directions, which is the same as Case 1. Thus, the acceleration amplitudes at 39 Hz were compared. The maximum acceleration amplitude error of the reduced model is 0.05 % in the *X* direction, 0.06 % in the *Y* direction, and 0.09 % in the *Z* direction, showing that the reduced model provides almost the same results as the full model.

Fig. 12 compares the displacement of the full model and the reduced model when the frequency is 39 Hz under Case 2 loading conditions. The total deformation (Fig. 12(a)) is 1.7×10^{-7} m for the full model and 1.69×10^{-7} m for the reduced model, with an error of only about 0.58 %. When comparing the displacements of the full model and the reduced model in each direction, errors of 0.82 % in *X* direction, 0.11 % in *Y* direction, and 4.08 % in *Z* direction occur, indicating that the displacements of the two models are almost the same.

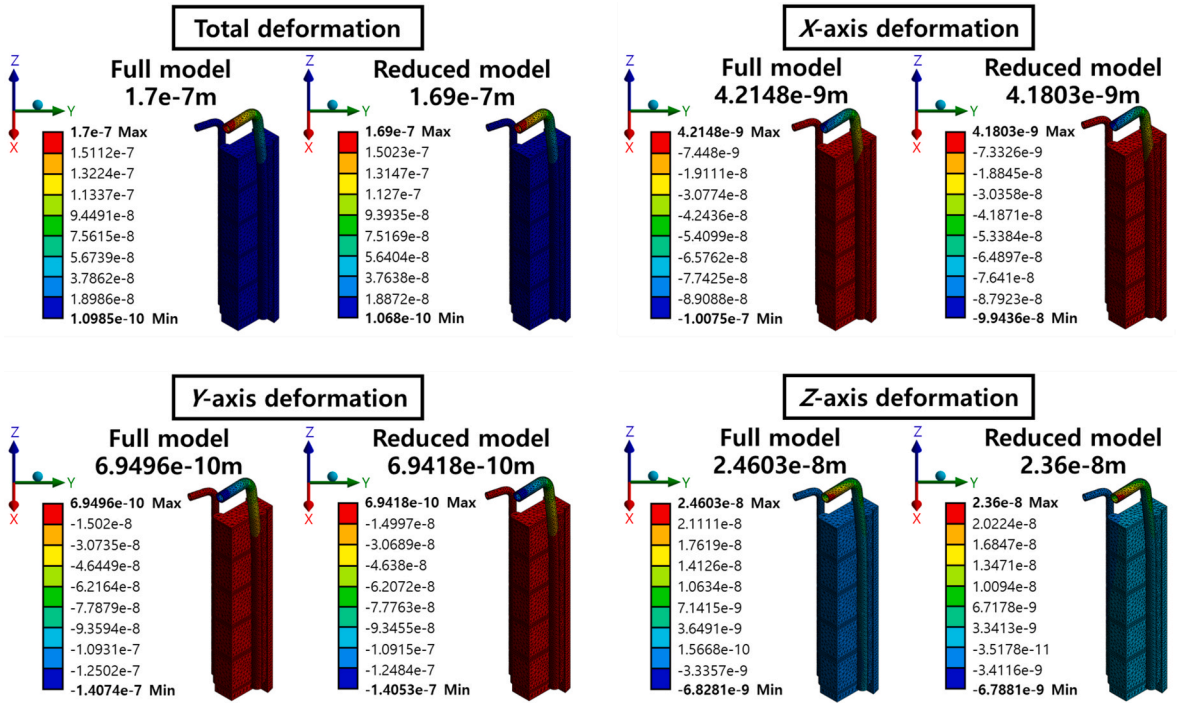

Fig. 12. Analysis results of deformation between full model and reduced model in Case 2 (a) total deformation (b) *X*-axis deformation (c) *Y*-axis deformation (d) *Z*-axis deformation (unit: m).

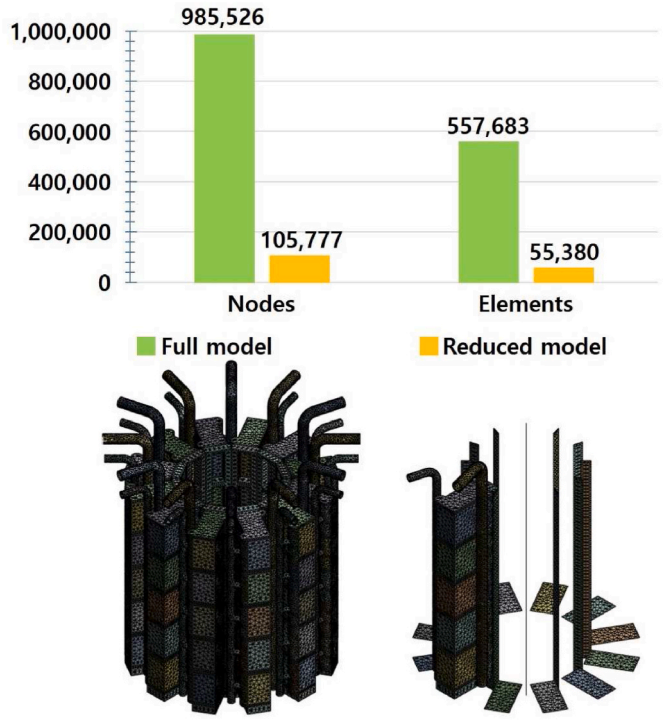

Fig. 13. FE model comparison of full model and reduced model.

4. Discussions: comparison of computational time between full model and reduced model

The computational accuracy of the reduced model was verified in Section 3. In this section, the computational time reduction effect of the reduced model was analyzed by comparing the calculation time when applying the reduced model and the full model.

Fig. 13 compares the number of nodes and elements of the reduced model and full model. Using a reduced model, the number of nodes can be reduced by about 9.32 times and the number of elements by about 10.07 times compared to the full model. Here, the full model is a model in which the 1st and 2nd sheets are simplified by applying the homogenization method [12]. Note that the entire model, which reflects the micro-channel shape, requires much more nodes and elements than the full model.

Fig. 14 compares the computational time of the reduced model and the full model. It can be seen that the reduced model has approximately 3.42 times faster calculation time in modal analysis and 4.59 times faster in frequency response analysis than the full model.

Modal analysis and frequency response analysis are essential analyses at the design stage, and even for a full model using only the homogenization method, the computational time takes about 2 h. If the analysis is performed with the entire model, much more time will be required. However, by applying the reduced model using both the homogenization method and the sub-structuring method, the computational time could be dramatically reduced to about 30 min.

In the preliminary design stage, design changes are frequently required for the steam generators. Therefore, it is considered to be very effective in design work if the structural integrity assessment of the PCSG assembly is performed by applying the reduced model presented in this research.

5. Conclusions

In this paper, a procedure for creating a reduced model of PCSG assembly was presented by applying the homogenization and sub-structuring methods. Then, it was shown that the seismic analysis time can be significantly decreased by applying the reduced model.

Creation of the reduced model proceeded in the following order.

(1) The homogenization method was applied to a sheet assembly in which the same micro-channel shape was repeated numerous times.
(2) The homogenized sheet assembly was assembled with a top plate, a bottom plate, a feedwater header and a steam header to form a simplified PCSG unit block.
(3) 5 simplified PCSG unit blocks, a feedwater pipe, a steam pipe, and a support structure were assembled to form a PCSG module set.
(4) 12 PCSG module sets were arranged in a circular pattern to create the full model of PCSG assembly.
(5) A reduced model of PCSG assembly is obtained by applying the sub-structuring method to one PCSG module set among the full model of PCSG assembly.

After obtaining the reduced model of PCSG assembly, modal analysis and frequency response analysis were then performed to validate the accuracy of the reduced model to which the homogenization and sub-structuring methods were applied. The analysis results were compared with the full model and it was confirmed that the reduced model provided almost the same analysis results as the full model.

To verify the computational efficiency of the reduced model, the computational time was then compared with the full model, and it was confirmed that the modal analysis time was reduced by 3.42 times and the frequency response analysis time was reduced by 4.59 times. Here, the full model is a model to which only the homogenization method is applied and the sub-structuring method is not applied. When the computational time of the reduced model is compared with the entire model that reflects the actual shape, the computational efficiency of this model can be even more highlighted. It is believed that this reduced model will have high utility in the design stage where shape changes

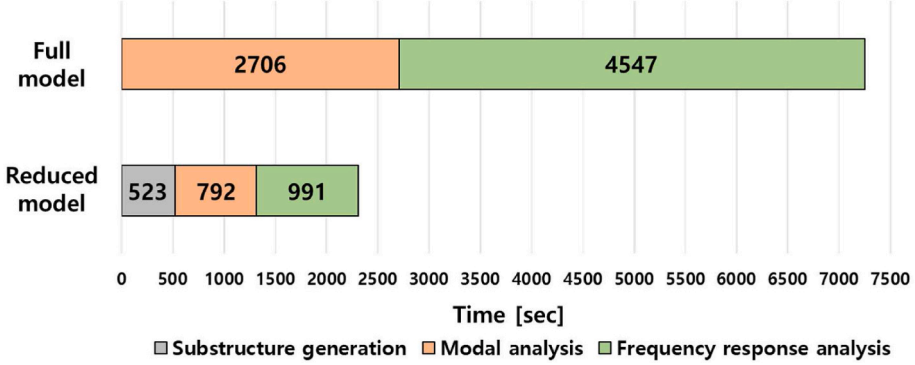

Fig. 14. Comparison of computational time between full model and reduced model.

occur frequently.

Declaration of competing interest

The authors declare that they have no known competing financial interests or personal relationships that could have appeared to influence the work reported in this paper.

Acknowledgements

This work was supported by the National Research Foundation of Korea (NRF) grant funded by the Korea government (MSIT) (NRF-2020M2D7A1079180 and RS-2023-00278230).

References

[1] Y.W. Kim, Basic Design Report for SMART Steam Generator, Korea Atomic Energy Research Institute, 2002. KAERI/TR-2127/2002.
[2] L. Liu, J. Fan, Technology readiness assessment of small modular reactor (SMR) designs, Prog. Nucl. Energy 70 (2014) 20–28.
[3] H.O. Kang, H.S. Han, Y.J. Kim, K.K. Kim, Thermal-hydraulic design of a printed-circuit steam generator for integral reactor, KSFM J. Fluid, March. 17 (2014) 77–83.
[4] S.W. Seo, J.Y. Lee, S.J. Kim, Status of Manufacturing Experimental Apparatus to Investigate SWR Phenomenon in the PCSG, Transactions of the Korean Nuclear Society Spring Meeting, Jeju, Korea, 2019.
[5] J.S. Kwon, D.H. Kim, S.G. Shin, J.I. Lee, S.J. Kim, Assessment of thermal fatigue induced by dryout front oscillation in printed circuit steam generator, Nucl. Eng. Technol. 54 (2022) 1085–1097.
[6] S.J. Kim, T.W. Kim, Design methodology and computational fluid analysis for the printed circuit steam generator, J. Mech. Sci. Technol. 34 (2020) 5303–5314.
[7] Y.J. Lee, S.J. An, S.W. Lim, 1-D PCSG model development for preliminary safety analysis of SMART Plus, in: Transactions of the Korean Nuclear Society Virtual Autumn Meeting, 2021.
[8] C.W. Shin, H.C. No, Experimental study for pressure drop and flow instability of two-phase flow in the PCHE-type steam generator for SMRs, Nucl. Eng. Des. 318 (2017) 109–118.
[9] X. Yuan, L. Yang, Z. Shang, Experimental and numerical investigation on flow boiling in a small semi-circular channel of plate once-through steam generator, Heat Tran. Eng. 43 (2022) 208–222.
[10] I.H. Kim, H.C. No, J.I. Lee, B.G. Jeon, Thermal hydraulic performance analysis of the printed circuit heat exchanger using a helium test facility and CFD simulations, Nucl. Eng. Des. 239 (2009) 2399–2408.
[11] A.D. Ronco, A. Cammi, S. Lorenzi, Preliminary analysis and design of the heat exchangers for the molten salt Fast reactor, Nucl. Eng. Technol. 52 (2020) 51–58.
[12] G.G. Youn, W.J. Jang, Y.J. Jeon, K.H. Lee, G.M. Lee, J.S. Lee, S. Chang, Structural integrity assessment procedure of PCSG unit block using homogenization method, Nucl. Eng. Technol. 55 (2023) 1365–1381.
[13] E. Sanchez-Palencia, Non-homogenous media and vibration theory, in: Volume 127 of Lecture Notes in Physics, Springer, Berlin, 1980.
[14] A. Benssousan, J.L. Lions, G. Papanicoulau, Asymptotic Analysis for Periodic Structures, AMS Chelsea Publishing, Rhode Island, 2010.
[15] D. Cioranescu, J.S.J. Paulin, Homogenization in open sets with holes, J. Math. Anal. Appl. 71 (1979) 590–607.
[16] J.M. Guedes N. Kikuchi, Preprocessing and postprocessing for materials based on the homogenization method with adaptive finite element methods, Comput. Methods Appl. Mech. Eng. 83 (1990) 143–198.
[17] M.P. Bendsøe, N. Kikuchi, Generating optimal topologies in structural design using a homogenization method, Comput. Methods Appl. Mech. Eng. 71 (1988) 197–224.
[18] Y.Y. Kim, Theory and Applications of Elasticity, second ed., Munundang, Seoul, 2009.
[19] S. Chang, S. Yang, H. Shin, M. Cho, Multiscale homogenization model for thermoelastic behavior of epoxy-based composites with polydisperse SiC nanoparticle, Compos. Struct. 128 (2015) 342–353.
[20] S. Weng, H. Zhu, Y. Xia, Substructuring method for eigensolutions, in: Substructuring Method for Civil Health Monitoring, Engineering Applications of Computational Methods vol. 15, Springer, Singapore, 2023.
[21] P. Seshu, Substructuring and component mode synthesis, Shock Vib. 4 (3) (1997) 199–210.
[22] S. Chang, M. Cho, Dynamic-condensation-based reanalysis by using the Sherman-Morrison-Woodbury formula, AIAA J. 59 (3) (2021) 905–911.
[23] H. Chung, Z. Du, Optimized design of multi-material cellular structures by level-set method with Guyan reduction, J. Mech. Des. 143 (10) (2021) 101702.
[24] H. Sung, S. Chang, M. Cho, Component model synthesis using model updating with neural networks, Mech. Adv. Mater. Struct. 30 (2) (2023) 400–411.
[25] K. Ahn, K.H. Lee, J.S. Lee, S. Chang, 3D-based equivalent model of SMART control rod drive mechanism using dynamic condensation method, Nucl. Eng. Technol. 54 (3) (2022) 1109–1114.
[26] K.H. Lee, R.W. Hagos, S. Chang, J.G. Kim, Multiphysics mode synthesis of fluid-structure interaction with free surface, Eng. Comput. 39 (4) (2023) 2889–2904.
[27] L. Mapa, F. das Neves, G.P. Guimaraes, Dynamic Substructuring by the Craig-Bampton method applied to frames, J. Vib. Eng. Technol. 9 (2021) 257–266.
[28] W. Hurty, Dynamic analysis of structural systems using component modes, AIAA J. 3 (4) (1965) 678–685.
[29] R. Guyan, Reduction of stiffness and mass matrices, AIAA J. 3 (2) (1965) 380.
[30] R.R. Craig, M.C.C. Bampton, Coupling of substructures for dynamic analysis, AIAA J. 6 (7) (1968) 1313–1319.
[31] Y. Wang, R. Palacios, A. Wynn, A method for normal-mode-based model reduction in nonlinear dynamics of slender structures, Comput. Struct. 159 (2015) 26–40.
[32] J.M. Mencik, D. Duhamel, A wave-based model reduction technique for the description of the dynamic behavior of periodic structures involving arbitrary-shaped substructure sand large-sized finite element models, Finite Elem. Anal. Des. 101 (2015) 1–14.
[33] F. Ola, P. Kent, S. Goran, Reduction methods for the dynamic analysis of substructure models of lightweight building structures, Comput. Struct. 138 (2014) 49–61.
[34] W. Chen, D. Wang, Y. Zhang, Seismic fragility analysis of nuclear power plants based on substructure method, Nucl. Eng. Des. 382 (2021) 111389.
[35] Korea Electric Association, M.D. Kepic, Material Properties (SI Unit), 2015 Edition, 2015.
[36] The American Society of Mechanical Engineers, ASME BPVC Sec. II Part D: Properties (Metric), 2015 Edition, 2015.